A Multiple Stimuli-Sensitive Low-Molecular-Weight Gel with an Aggregate-Induced Emission Effect for Sol–Gel Transition Detection

Hao Wang, Qihong Liu, Yalong Hu, Miaochang Liu, Xiaobo Huang, Wenxia Gao,* and Huayue Wu[a]

A low-molecular-weight gel (LMWG) with a hydrazone moiety and an aggregate-induced emission (AIE) unit was fabricated; the self-assembly and disassembly of the LMWG under different stimuli conditions were studied. The LMWG exhibited multiple stimuli sensitivity with temperature, light, ions, and ionic strength. The hydrazone was integrated into the gelator to act as ion sensing sites and hydrogen bond donor groups to fulfil the task of ion recognition of Ni^{2+}, BH_4^-, and OH^-, as well as ion-controlled reversible sol–gel recovery by adding H^+ for deprotonation; it also broke under UV irradiation to evoke light-sensitivity. In addition, the sol–gel transition of the gel was detected by the AIE effect. The research provided an effective strategy in fabricating multiple stimuli-sensitive LMWGs for potential biomedical applications.

1. Introduction

Stimuli-sensitive low-molecular-weight gels (LMWGs) with unique properties have attracted great interest from chemists and materials scientists and have been utilized in sensors,[1,2] environmental pollution control,[3] tissue engineering,[4–6] and drug-delivery systems.[7,8] Temperature, ion, ion strength, and light could all be used as stimuli to induce the self-assembly, disassembly, and other behaviors and functions of LMWGs. The characteristics and conditions of sol–gel transitions were the most important aspects for stimuli-sensitive LMWG investigations. Visualization and rheological measurements were the commonly used characterizations to confirm gel formation.

The research of thermal-sensitive LMWGs was focused on the temperature of phase transition. The gels could be controlled reversibly or irreversibly in response to thermal stimuli.[9] The temperature for the gel–sol transition was termed T_{gel}; this temperature was the watershed for the properties of gel or sol to the soft matter. The essence of the sol–gel transition was attributed to the aggregation behavior change of gelators. The gelation process of this aggregation could be visualized by aggregation-induced emission (AIE) fluorogens, as reported by Tang and co-workers.[10–12] In this research, the triphenylamine units were involved in the gelators to monitor the sol–gel transition to multiple stimuli.

To ion- and ion-strength-responsive LMWGs, the ion response and selective recognition were the intrinsic essence to induce the formation of gels. Both anions, including OH^-, F^-, AcO^-, and $H_2PO_4^-$,[13] and cations, such as H^+, Hg^{2+}, Ag^+, Cd^{2+}, and Fe^{3+},[14] could trigger the self-assembly and disassembly of the gelators. Rare LMWGs were detected the sol–gel transition with the adjustment of anions and cations at the same time.

For light-responsive LMWGs, photoisomerization, photodimerization, and photopolymerization were all the factors that induced bond formation or cleavage of photoresponsive gelators for fabricating gels.[15] The isomerization of azobenzene and stilbenes was the most widely used in gelators to result in gel–sol or sol–gel transitions.[16] Different from isomerization of azobenzene and stilbenes, dimerization of coumarin-based gels occurred under the irradiation of 300 nm UV light;[17] the gelation was disrupted for the photocleavage of carboxy-2-nitrobenzyl or pyridine-ruthenium bond under UV irradiation.[18,19]

To date, a large number of gels with one stimulus response, including pH, photochemical, heat, or ions, have been reported.[20] However, LMWGs with multiple stimuli sensitivity at the same time have rarely been studied, owing to difficulties in the integration of the multiple sensitivity units in the same gelator. A LMWG with multiple stimuli sensitivity based on the same functional group of hydrazone has been developed in this work to achieve light, heat, and ion responses (Figure 1 A). The self-assembly and disassembly of the gelators under different stimuli conditions were studied. Moreover, the AIE of the gelators was found to be used as the probe to detect the sol–gel transition of the LMWG.

[a] H. Wang, Q. Liu, Y. Hu, M. Liu, X. Huang, Dr. W. Gao, H. Wu
College of Chemistry and Materials Engineering
Wenzhou University
Chashan Town, 325000 Wenzhou City, Zhejiang Province (P. R. China)
E-mail: wenxiag@wzu.edu.cn

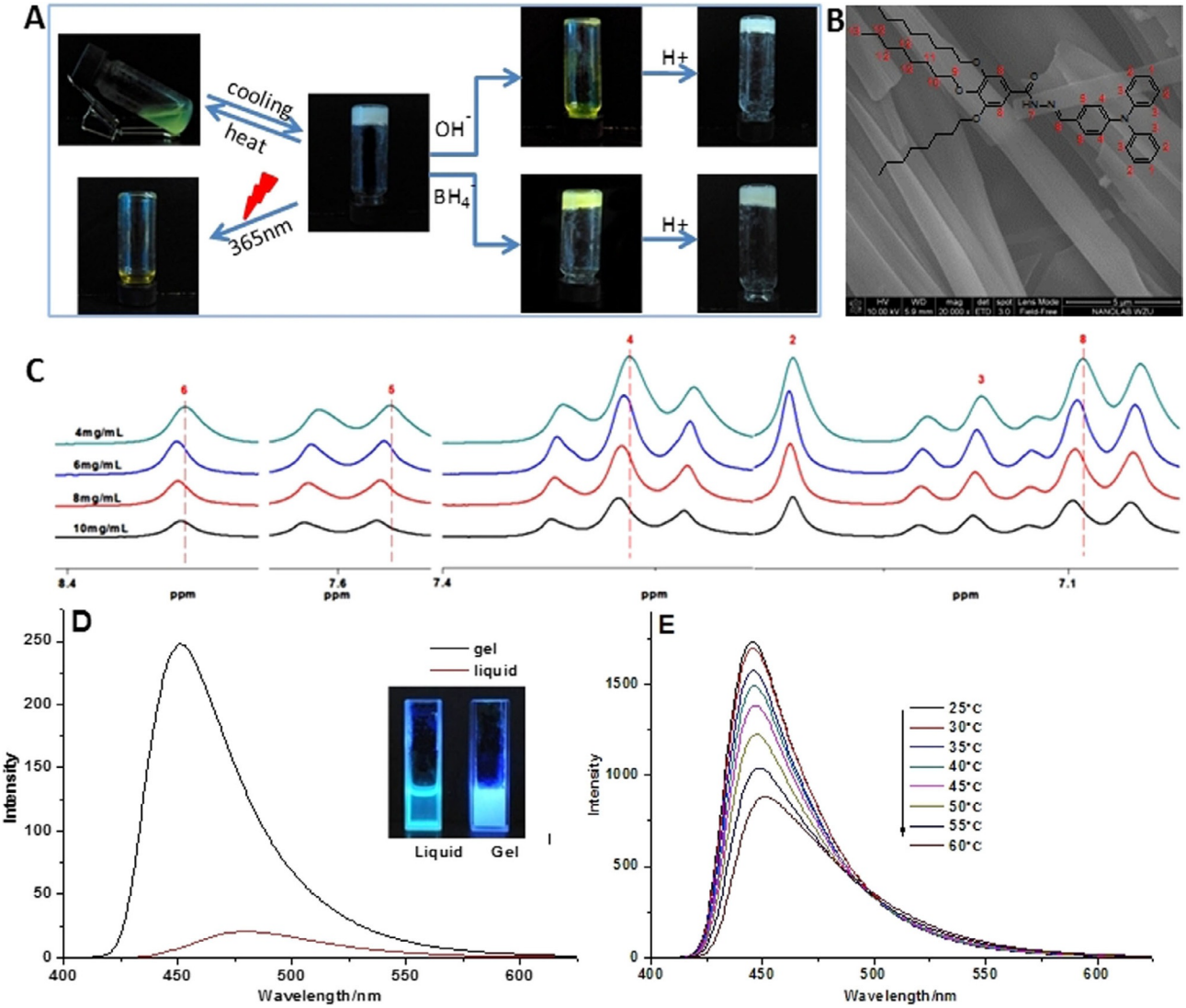

Figure 1. The gel response to various stimuli (A); SEM image of xerogel (B); ^{1}H NMR spectra of different concentrations of the gelator in DMSO (C); fluorescence spectra of sol and gel of the gelator in the mixed solvent (DMSO/H_2O = 10:1), λ_{ex} = 370 nm (D); fluorescence spectra of the gelator in the mixed solvent (DMSO/H_2O = 10:1) (14.0 mg mL^{-1}) at different temperatures, λ_{ex} = 370 nm (E).

2. Results and Discussion

The synthesis of gelator is presented in Scheme 1 and the characterization of the gelator are shown in Figures S1–S9 of the Supporting Information. The critical gelation concentration (CGC) of the gelator was 10.0 mg mL^{-1}. The fibers with 0.5–3.0 μm diameters of the air-dried gel were observed by using SEM (Figure 1 B). The π-conjugated moieties containing gallic acid and triphenylamine contributed to the gelation.[21] The π–π stacking interaction between gelators was characterized by fluorescence spectra (Figure S10). The fluorescence spectra of the gelator were measured at different concentrations, and the increase in fluorescence was attributed to the increase in gelator concentration from 1 to 30 μg mL^{-1}. The fluorescence quenching occurred once the concentration was higher than 30 μg mL^{-1}. The fluorescence quenching indicated the formation of π–π stacking.[22] The ^{1}H NMR spectra showed the gradual high-field shift of protons upon increasing the concentration of gelator (Figure 1 C). The protons of benzene shifted downfield from 7.34 to 7.36 ppm and 7.58 to 7.60 ppm when the concentration of gelator increased from 4 mg mL^{-1} (sol) to

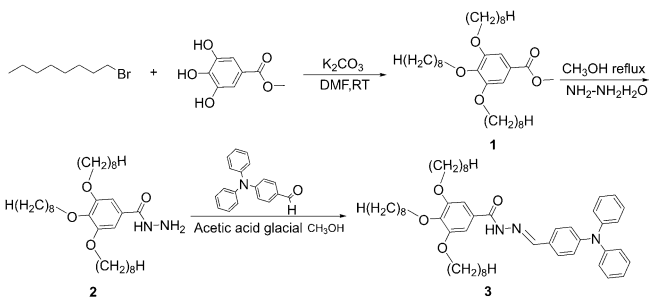

Scheme 1. The synthesis of gelator (compound **3**).

10 mg mL^{-1} (gel). These results implied that the π–π stacking of benzene units in the gel was strengthened with increasing concentration. The chemical shift of proton in imine (–*CH*=*N*–) was also affected in the gelation, which shifted downfield from 8.36 to 8.38 ppm, implying the driving forces were van der Waals forces and π–π interactions in the gelation.[23]

The π-conjugated moiety of triphenylamine in the gelator not only improved the gelation property, but also induced AIE to detect the stimuli-sensitive sol–gel transition. The AIE behavior of the gelator was evaluated by using a fluorescence assay (Figure 1 D). When the gelator molecules self-assembled into a gel, the intramolecular motion and rotations of triphenylamine were restricted to suppress the energy consumption and resulted in the fluorescence emergence.[23] The AIE effect was further used to detect the thermal-sensitive sol–gel transition (Figure 1 E). The gelation could occur at room temperature, and the fluorescence intensity of the gel gradually decreased as the gel gradually turned to sol when increasing the temperature.

The fluorescence response of the gel to cations and anions was investigated, as shown in Figure 2. Selectivity of cations was examined by addition of various cations by adding their fluoride salts (Ba^{2+}, Li^{+}, Al^{3+}, K^{+}, Ca^{2+}, Sr^{2+}, Gd^{3+}, Cr^{3+}, Ag^{+}, Mg^{2+}, Zn^{2+}, Ni^{2+}) to the solution of the gelator (Figure 2 A). The intensity of the fluorescence decreased after the addition of some metal cations, especially after addition of Ni^{2+}, as fluorescence quenching appeared. With the diffusion of metal ions into the gel, the supramolecular metallogel might form, such as the exemplary gelator–Ni^{2+} complex shown in Figure 3 A. The recognition of 18 anionic sodium salts for the gelator was also investigated (Figure 2 B). The selective recognition of BH_4^- showed a dramatic color change, both in solution and in the gel state (Figure 2 B, Figure 3 D), and the fluorescence intensity also decreased dramatically (Figure 2 B). It was interesting that

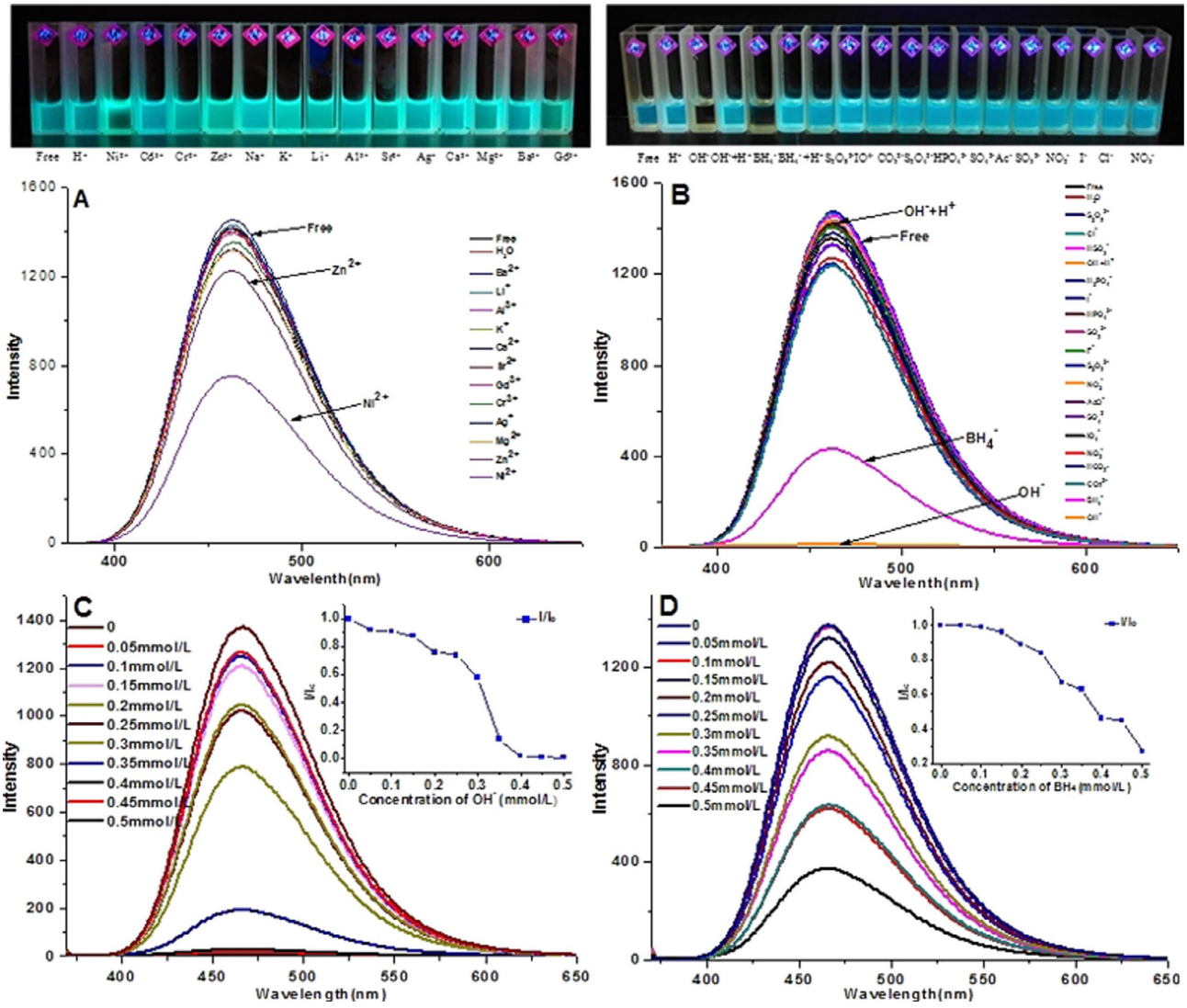

Figure 2. Fluorescence spectra of the gelator in mixed solvent (DMSO/H_2O = 10:1) (5.0×10^{-3} mmol L^{-1}) with the addition of different ions: with addition of different cations at 0.5 mmol L^{-1} (A); with the addition of different anions at 0.5 mmol L^{-1} (B); with different concentrations of sodium hydroxide (C); with different concentrations of sodium borohydride (D). The insert shows the fluorescent intensity ration I/I_o, where I = fluorescent intensity of gelator upon addition of OH^- or BH_4^- and I_0 = fluorescent intensity of gelator.

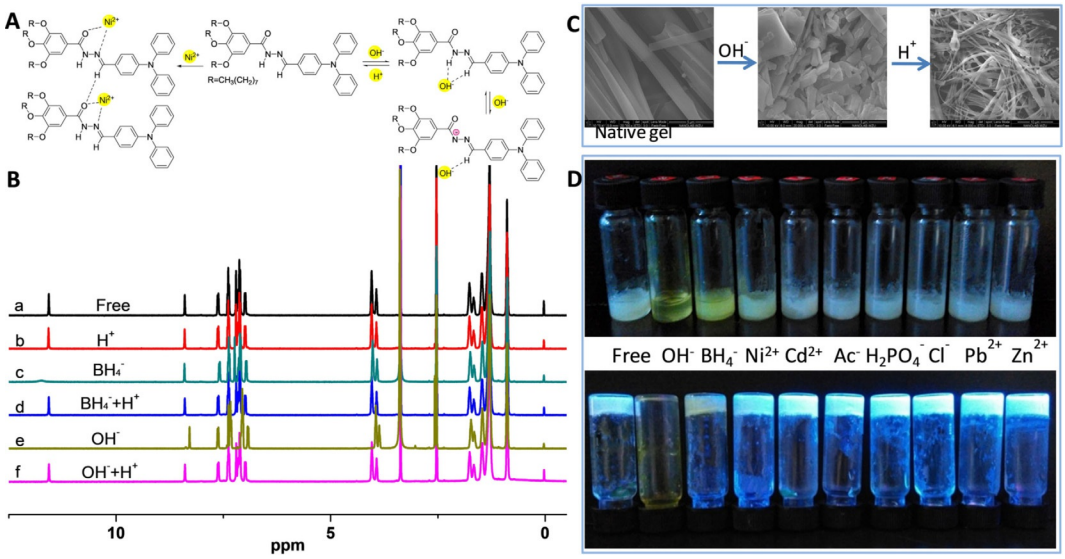

Figure 3. A possible mechanism of gel response to Ni^{2+} and OH^-, and recovery upon adding H^+ (A); ^1H NMR spectra of gelator (5 mg mL^{-1}) in D_2O upon the addition of ions (B): free (a), H^+ (b), BH_4^- (c), H^+ (d) to the sample with addition of BH_4^-; OH^- (e), H^+ (f) added to the sample with addition of OH^-. SEM images (C) of gel, gel treated with OH^- in situ, gel treated with OH^- in situ and then added H^+. Images of gel response to various ions (D).

no gel–sol phase transition was observed during the recognition process of Ni^{2+} and BH_4^-; even the architecture of the gel was changed greatly from nanofibers to nanobelts or segments (Figure S11). The recognition of OH^- was more special. The gel fulfilled OH^- recognition through a reversible gel–sol phase transition with dramatic fluorescence quenching (Figure 2B, Figure 3D). The response rate was slow at the beginning for the gel in contact with the ionic solution, and then the response rate increased rapidly (Figure S12). The color and the microstructure could be recovered by adding H^+. OH^- could be competitively bound to the hydrazone groups, which acted as anion binding as well as self-assembly sites (Figure 3A).[24] Therefore, the phase changed for the disassembly of gelator upon the addition of OH^- and reassembly into a gel with the addition of H^+ to consume OH^- (Figure 3C).

A further anion recognition reaction mechanism was observed by using ^1H NMR spectroscopy, as shown in Figure 3B. Before the addition of the anions, the chemical shifts of the –*CH*=*N*– proton appeared at 8.36 ppm. After adding 2 equivalents of OH^-, the resonances of –*CH*=*N*– protons disappeared, indicating the formation of N–H–OH and N=C–H–OH hydrogen bonds and a subsequent deprotonation process. Owing to the deprotonation, the gel was broken with a color change from white to yellow for the intermolecular hydrogen bonds. The deprotonation resulted in the disassembly of the gel. With further H^+ addition, the signal for the –*CH*=*N*– protons appeared again, with re-gelation then occurring immediately, as also revealed by the color. The microstructure of the gel also experienced the process of destruction upon addition of OH^- and subsequent recovery by addition of H^+ (Figure 3C). According to the ^1H NMR results, we presumed the mechanism of anion-induced gel–sol transition. According to these results, we inferred that the gel showed a different response to cations and anions. With the same concentration of gelator and identical excitation conditions, the fluorescent intensity decreased when adding OH^- (Figure 2C) and BH_4^- (Figure 2D). When the concentration of OH^- reached 50-times that of the gelator, the fluorescent intensity decreased dramatically to 58% of initial intensity (I_o), and it further decreased to 14% of I_o when the concentration of OH^- reached 70-times that of the gelator (insert plot in Figure 2C). In comparison, the gelator showed less sensitivity to BH_4^- than OH^-. Other anions (such as I^-, $H_2PO_4^-$, SO_4^{2-}, NO_3^-, HCO_3^-, CO_3^{2-}, and so on) and cations (such as Ba^{2+}, Li^+, Al^{3+}, K^+, Ca^{2+}, Sr^{2+}, Gd^{3+}, Cr^{3+}, Ag^+, Mg^{2+}) did not lead to any similarly obvious responses. Therefore, this gel could selectively recognize the cation of Ni^{2+} and anions of BH_4^- and OH^-. Reversible sol–gel could be adjusted by adding H^+.

The photocleavable property of the gel was also investigated, as shown in Figure 4. The gel gradually transitioned into sol under UV irradiation over 120 h (365 nm, 75 mW cm^{-2}), and the solution turned yellow (Figure 4A); the fluorescence intensity was weakened greatly (Figure 4C). It was found that the imide group in the hydrazone moiety of the gelator was broken to generate 4-diphenylaminobenzaldehyde in the process of illumination. (Figure 4B). The concentration of the gelator and the decomposition products during exposure to the light were tracked by using high-performance liquid chromatography (HPLC) (Figure S13, Figure 4D); two peaks with retention times $Rt = 2.58$ min and $Rt = 12.35$ min were found. The corresponding compound with $Rt = 2.58$ min was confirmed by ^1H NMR and ^{13}C NMR spectroscopy to be 4-diphenylbenzaldehyde, as shown in Figure S14. This confirms the gel photolysis, and that the gelator was photocleaved gradually into a 4-diphenylamine benzaldehyde upon exposure to light. The gelator in solution was more sensitive to UV light and 94.66 mg mL^{-1} of gelator solution was broken within 3.5 h to 24.3 mg mL^{-1}. The gel photolysis rate was much slower, which

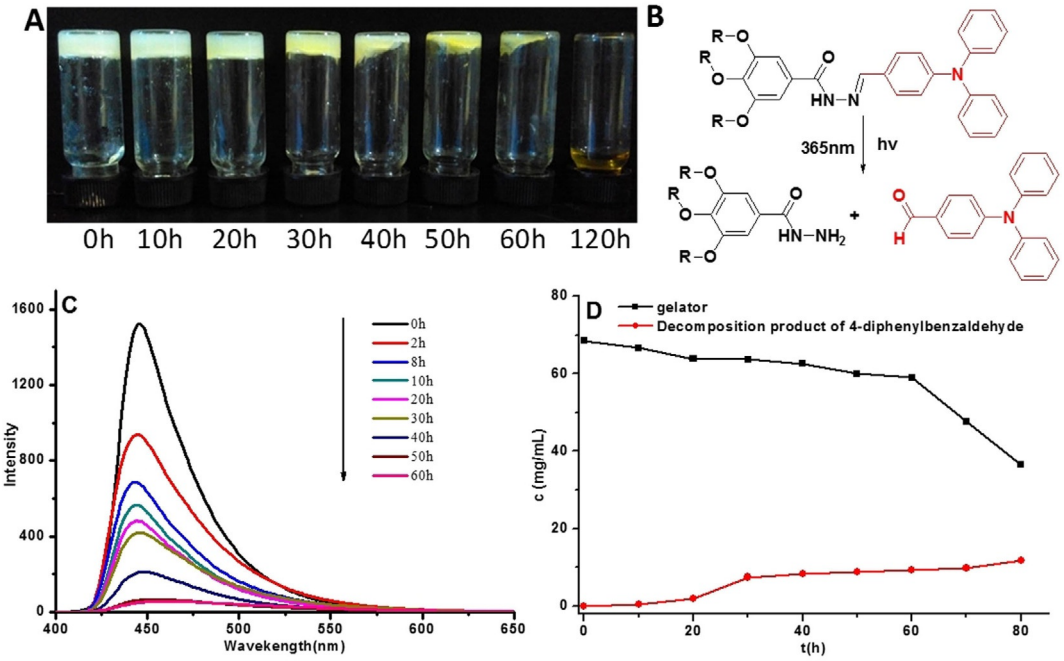

Figure 4. Images of gel exposed to light for different lengths of time (A), photocleavage mechanism of the gel (B), fluorescence spectra of gel during UV light exposure (365 nm, 75 mW cm^{-2}) (C), and the concentration of gelator and decomposition products during exposure to UV light (D).

was attributed to the enhanced molecular interaction in the gel state, which weakened the degradation speed of the gelator exposed to UV light (Figure S15, S16). The microstructure of the gel changed in the process of illumination. The nanofibers of the gel broke into small segments first, and then the gel gradually transferred into sol with further illumination (Figure S17).

3. Conclusions

A new LMWG with a hydrazone group and triphenylamine units was fabricated to achieve multiple sensitivity to the stimuli of temperature, light, and ions. Hydrazone was integrated into the gelator to act as ion-sensing sites and hydrogen bond donor groups for ion recognition of Ni^{2+}, BH_4^-, and OH^-; it also breaks down under UV irradiation to evoke light sensitivity. The sol–gel transition could be recovered for the deprotonation of OH^- by further adding H^+. In addition, the sensitive sol–gel transition could be tracked by the fluorescence of the AIE effect of triphenylamine units in the gelator. The LMWG exhibited a satisfactory response to light, heat, ions, and ion-controlled reversible sol–gel transition with AIE. This research provides an effective strategy to fabricate multiple stimuli-sensitive LMWGs for potential biomedical applications.

Experimental Section

Material and Methods

1-Bromooctane, methyl gallate, hydrazine hydrate, and potassium carbonate were purchased from Shanghai SA Chemical Technology (Energy Chemical) Co., Ltd. 4-(*N*, *N*-Diphenylamino) benzaldehyde was purchased from Shanghai Meryer Chemical Technology Co., Ltd. The solvents used in the HPLC measurements were of chromatographic grade, and all solvents used in the remaining experiments were of analytical grade. All solvents and reagents were used without further treatment.

General Techniques

^{1}H and ^{13}C NMR spectroscopy were both performed on a Bruker 500 spectrometer operating at 500 MHz (^{1}H NMR) and 125 MHz (^{13}C NMR). Tetramethylsilane (TMS) was used as an internal standard and DMSO (d_6) was used as the solvent. Mass spectrometric analysis was performed on a Bruker microTOF-QII HR-MS. Scanning electronic microscopy (SEM) images were taken on a Nova Nano SEM 200 scanning electron microscope. Transmission HPLC measurements were taken on an Agilent 1120 type liquid instrument using an Inertsil ods-sp C18 chromatographic column. UV spectra were recorded on a UV2501PC spectrometer (Shimadzu).

Synthesis of Compound 1

Methyl gallate (9.21 g, 50 mmol) and anhydrous potassium carbonate (41.5 g of 300 mmol) were added to 150 mL of dried dimethyl formamide. 1-Bromooctane (36.6 g, 165 mmol) was added dropwise under nitrogen at 80 °C for 6 h. The reaction was monitored by using thin-layer chromatography. After the reaction was completed, the solution was cooled to room temperature, 500 mL of deionized water was added, followed by extraction with diethyl ether. The ether phase was dried over anhydrous sodium sulfate, filtered, and evaporated to remove the diethyl ether. The crude product was purified by using silica gel column chromatography (ethyl acetate: petroleum ether = 1:30) to give compound **1** (24.3 g, 46.7 mmol, yield 93.3 %) as a yellow liquid. ^{1}H NMR (500 MHz, [d_6]DMSO, TMS) δ (ppm):7.19 (s, 2 H), 3.99 (s, 4 H), 3.82 (s, 3 H, J = 6.5), 1.72 (m, 4 H), 1.63 (m, 2 H), 1.44 (m, 6 H), 1.26 (s, 24 H),

0.86 (t, 9H, $J=7.0$). ^{13}C NMR (125 MHz, [D_6]DMSO, TMS) δ (ppm) (165.74, 152.48, 141.32, 124.39, 107.39, 72.48, 68.52, 52.07, 31.24, 29.78, 28.68, 25.48, 22.04,13.84).

Synthesis of Compound 2

Compound **1** (7.81 g, 15 mmol) was dissolved in methanol. An excess of hydrazine hydrate was added dropwise and stirred at reflux for 12 h. When the reaction was complete, it was cooled to room temperature to obtain a white precipitate. Recrystallization of the crude product in methanol gave compound **2** (7.34 g, 14.1 mmol, yield 94%) as a white solid. ^{1}H NMR (500 MHz, [D_6]DMSO, TMS) δ (ppm): (9.67 s, 1H), (7.12 s, 2H), 4.46 (s, 2H), 3.96 (t, 4H, $J=6.5$), 3.87 (t, 2H, $J=6.5$), 1.71 (m, 4H), 1.62 (m, 2H), 1.43 (m, 6H), 1.29 (m, 24H), 0.86 (t, 9H, $J=7.0$); ^{13}C NMR (125 MHz, [d_6]DMSO, TMS) δ (ppm) (165.35, 152.18, 139.45, 128.04, 105.25, 72.35, 68.31, 31.21, 29.76, 28.71, 25.58, 22.07, 13.85).

Synthesis of Compound 3

Compound **2** (2.73 g, 5.25 mmol) and a catalytic amount of glacial acetic acid were dissolved in ethanol. 4-Diphenylaminobenzaldehyde (1.37 g, 5 mmol) was added dropwise and the reaction was stirred at reflux for 12 h. After the reaction was complete, the mixture was cooled to room temperature; a yellow–green solid was obtained, filtered, and recrystallized in ethanol to give compound **3** (3.34 g, 3.8 mmol, yield 86%). ^{1}H NMR (500 MHz, [d_6]DMSO, TMS) δ (ppm): 11.51 (s, 1H), 8.38 (s,1H), 7.60 (d, 2H, $J=5.0$), 7.36 (t, 4H, $J=10.0$), 7.18 (s, 2H), 7.11 (q, 6H, $J=10.0$), 6.97 (d, 2H, $J=5.0$), 4.02 (s, 4H), 3.91 (t, 2H, $J=5.0$), 1.74 (m, 4H), 1.64 (m, 2H), 1.45 (d, 6H, $J=5.0$), 1.26 (s, 24H), 0.86 (d, 9H, $J=5.0$); ^{13}C NMR (125 MHz, [d_6]DMSO, TMS) δ (ppm) (152.34, 146.54, 129.70, 128.28, 124.93, 123.97, 121.41, 72.47, 68.55, 31.20, 29.76, 28.83, 28.68, 25.58, 22.06, 13.87).

Acknowledgements

This work was supported by National Natural Science Foundation of China (No. 21672164, 21372177), Natural Science Foundation of Zhejiang Province (No. LY15B020001), and Xinmiao Talents Program (No. KZ15S12065, 2016R426062) of Zhejiang Province.

Conflict of Interest

The authors declare no conflict of interest.

Keywords: aggregate-induced emission effect · biomedical applications · low-molecular-weight gels · multiple stimuli sensitivity · sensing

[1] T. Yoshii, S. Onogi, H. Shigemitsu, I. Hamachi, *J. Am. Chem. Soc.* **2015**, *137*, 3360–3365.
[2] J. Zhang, C. Ou, Y. Shi, L. Wang, M. Chen, Z. Yang, *Chem. Commun.* **2014**, *50*, 12873–12876.
[3] B. O. Okesola, D. K. Smith, *Chem. Soc. Rev.* **2016**, *45*, 4226–4251.
[4] K. Vulicand, M. S. Shoichet, *J. Am. Chem. Soc.* **2012**, *134*, 882–885.
[5] E. C. Wu, S. G. Zhang, C. A. E. Hauser, *Adv. Funct. Mater.* **2012**, *22*, 456–468.
[6] S. Khetan, M. Guvendiren, W. R. Legant, D. M. Cohen, C. S. Chen, J. A. Burdick, *Nat. Mater.* **2013**, *12*, 458–465.
[7] M. A. Ramin, K. R. Sindhu, A. Appavoo, K. Oumzil, M. W. Grinstaff, O. Chassande, P. Barthelemy, *Adv. Mater.* **2017**, *29*, 1605227.
[8] Y. Shi, Z. Wang, X. Zhang, T. Xu, S. Ji, D. Ding, Z. Yang, L. Wang, *Chem. Commun.* **2015**, *51*, 15265–15267.
[9] H. Danjo, K. Hirata, S. Yoshigai, I. Azumaya, K. Yamaguchi, *J. Am. Chem. Soc.* **2009**, *131*, 1638–1639.
[10] J. Luo, Z. Xie, J. W. Y. Lam, L. Cheng, H. Chen, C. Qiu, H. S. Kwok, X. Zhan, Y. Liu, D. Zhu, B. Z. Tang, *Chem. Commun.* **2001**, *0*, 1740–1741.
[11] S. Liu, Y. Cheng, H. Zhang, Z. Qiu, R. T. K. Kwok, J. W. Y. Lam, B. Z. Tang, *Angew. Chem. Int. Ed.* **2018**, *57*, 6274–6278; *Angew. Chem.* **2018**, *130*, 6382–6386.
[12] Z. Wang, J. Nie, W. Qin, Q. Hu, B. Z. Tang, *Nat. Commun.* **2016**, *7*, 12033.
[13] J. W. Steed, *Chem. Soc. Rev.* **2010**, *39*, 3686–3699.
[14] A. Nuthanakanti, S. G. Srivatsan, *ACS Appl. Mater. Interfaces* **2017**, *9*, 22864–22874.
[15] C. D. Jones, J. W. Steed, *Chem. Soc. Rev.* **2016**, *45*, 6546–6596.
[16] Z. L. Pianowski, J. Karcher, K. Schneider, *Chem. Commun.* **2016**, *52*, 3143–3146.
[17] E. R. Draper, T. O. McDonald, D. J. Adams, *Chem. Commun.* **2015**, *51*, 12827–12830.
[18] E. R. Draper, D. J. Adams, *Chem. Commun.* **2016**, *52*, 8196.
[19] S. Theis, A. Iturmendi, C. Gorsche, M. Orthofer, M. Lunzer, S. Baudis, A. Ovsianikov, R. Liska, U. Monkowius, I. Teasdale, *Angew. Chem. Int. Ed.* **2017**, *56*, 15857–15860; *Angew. Chem.* **2017**, *129*, 16071–16075.
[20] Y. Zhang, Q. Lin, T. Wei, X. Qin, Y. Li, *Chem. Commun.* **2009**, *0*, 6074–6076.
[21] R. Das Mahapatra, J. Dey, *Langmuir* **2015**, *31*, 8703–8709.
[22] D. Maity, T. Govindaraju, *Eur. J. Inorg. Chem.* **2011**, *2011*, 5479–5485.
[23] V. M. Suresh, A. De, T. K. Maji, *Chem. Commun.* **2015**, *51*, 14678–14681.
[24] X. Yu, L. Chen, M. Zhanga, T. Yi, *Chem. Soc. Rev.* **2014**, *43*, 5346–5371.